AJNR

Comparison of MR Imaging, CT, and Angiography in the Evaluation of the Enlarged Cavernous Sinus

William L. Hirsch, Jr., Frank G. Hryshko, Laligam N. Sekhar, James Brunberg, Emanuel Kanal, Richard E. Latchaw and Hugh Curtin

AJNR Am J Neuroradiol 1988, 9 (5) 907-915
http://www.ajnr.org/content/9/5/907

Comparison of MR Imaging, CT, and Angiography in the Evaluation of the Enlarged Cavernous Sinus

William L. Hirsch, Jr.[1]
Frank G. Hryshko[1]
Laligam N. Sekhar[2]
James Brunberg[1]
Emanuel Kanal[1]
Richard E. Latchaw[1]
Hugh Curtin[1]

Twenty-one patients with enlargement of the cavernous sinus were studied with CT and MR imaging. Eighteen of the patients also had cerebral angiography. MR was superior to CT in differentiating parasellar aneurysms from neoplastic masses. MR was also superior to both CT and angiography in defining the relationships of cavernous sinus neoplasms to the internal carotid artery, pituitary gland, optic chiasm, infundibulum, and fifth cranial nerves. Only in the definition of bone erosion or hyperostosis was MR inferior to another method (CT).

We conclude that MR should be the initial diagnostic study in patients with symptoms of a parasellar mass, with supplementation when necessary by CT and angiography.

The anatomy of the cavernous sinus is complex and has been reviewed recently [1, 2]. In the past, masses of the cavernous sinus were rarely treated surgically because of potential bleeding from the cavernous venous plexus; injury to the internal carotid artery; or damage to cranial nerves III, IV, or VI. New surgical approaches, use of the surgical microscope, and intraoperative electromyographic monitoring of cranial nerve function have facilitated the surgical management of cavernous sinus lesions [3, 4].

The radiographic evaluation of patients with a suspected parasellar lesion is directed toward detecting the mass, determining if the mass is an aneurysm or neoplasm, and, if neoplastic, determining the relationship of the mass to surrounding structures. It is particularly important to differentiate neoplastic masses from cavernous sinus aneurysms, as treatment is radically different [5, 6]. A comparison of the efficacy of angiography, CT, and MR in the evaluation of parasellar lesions is the subject of this report.

Materials and Methods

Over a 20-month period, 21 masses that enlarged the cavernous sinus were studied with MR and CT; in 18 patients angiography was performed also. Seventeen of the masses were centered in the cavernous sinus. Four of the masses (three pituitary adenomas and one chondrosarcoma) were centered in the sella and involved the cavernous sinus secondarily. There was histologic confirmation of a neoplastic mass in 15 patients, angiographic and MR confirmation of four patients, and endocrinologic proof of a pituitary adenoma in one patient (Table 1). In one patient the diagnosis of a completely thrombosed cavernous aneurysm was based on CT and MR criteria alone. This presumed aneurysm could not be seen angiographically because of thrombosis of the aneurysm and the ipsilateral carotid artery. All imaging studies were done within 1 week of one another in 16 patients and within 1 month of one another in four patients. In one patient with a plexiform neurofibroma, CT and MR studies were performed 6 months apart.

CT was performed on a GE 9800 scanner* in 19 patients and on a Picker 1200 scanner† in two patients. Contrast material was administered to 20 patients by IV drip infusion. One patient did not receive contrast material owing to allergy. Coronal and axial CT scans were obtained in 13 patients. Axial images only were obtained in eight patients. The cavernous

This article appears in the September/October 1988 issue of *AJNR* and the November 1988 issue of *AJR*.

Received September 16, 1987; accepted after revision February 19, 1988.

[1] Department of Radiology, Presbyterian-University Hospital and University of Pittsburgh School of Medicine, DeSoto at O'Hara Sts., Pittsburgh, PA 15213. Address reprint requests to W. L. Hirsch, Jr.

[2] Department of Neurosurgery, Presbyterian-University Hospital and University of Pittsburgh School of Medicine, Pittsburgh, PA 15213.

***AJNR* 9:907–915, September/October 1988**
0195–6108/88/0905–0907

* General Electric Medical Systems, Milwaukee, WI.
† Picker International, Cleveland, OH.

TABLE 1: Summary of Patients with Parasellar Masses and Method of Diagnosis

Case No.	Age	Gender	Diagnosis	Confirmation
1	63	M	Meningioma	Histology
2	63	F	Meningioma	Histology
3	52	M	Meningioma	Histology
4	41	F	Recurrent meningioma	Histology
5	56	F	Recurrent meningioma	Histology
6	63	M	Recurrent meningioma	Histology
7	36	F	Recurrent meningioma	Histology
8	49	M	Pituitary adenoma	Histology
9	72	F	Pituitary adenoma	Histology
10	48	M	Pituitary adenoma	Elevated prolactin
11	31	M	Nerve sheath tumor	Histology
12	49	F	Fifth nerve sheath tumor	Histology
13	65	M	Adenocystic carcinoma	Histology
14	25	M	Chondrosarcoma	Histology
15	3	M	Plexiform neurofibroma	Histology
16	77	M	Metastatic renal cell carcinoma	Histology
17	30	F	Cavernous carotid aneurysm	MR, angiography
18	31	M	Cavernous carotid aneurysm	MR, angiography
19	80	F	Cavernous carotid aneurysm	MR, angiography
20	49	F	Thrombosed aneurysm	MR
21	66	F	Bilateral cavernous carotid aneurysms	MR, angiography

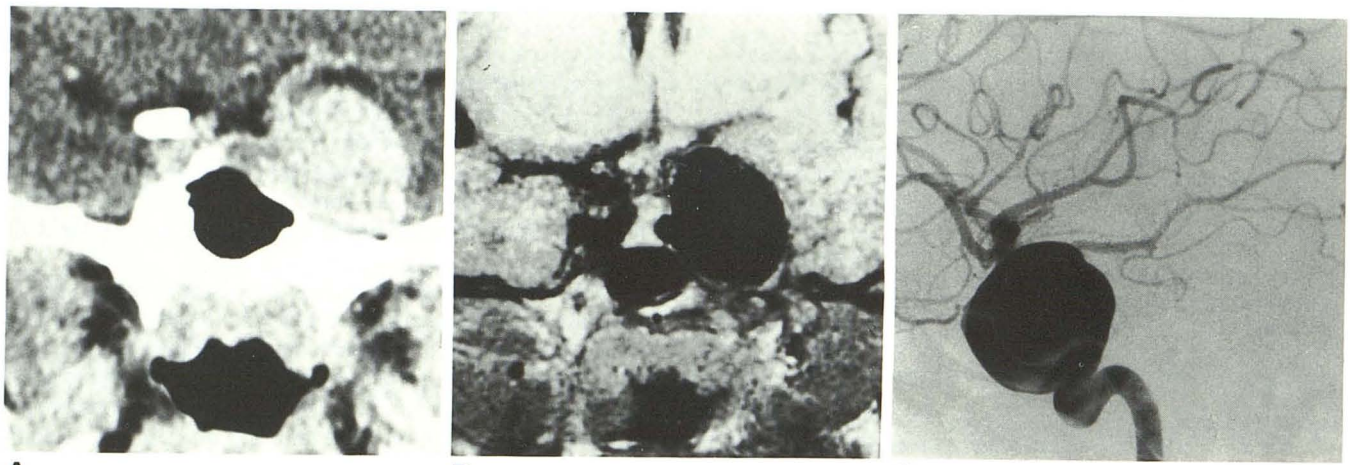

Fig. 1.—Case 17: Giant aneurysm in 30-year-old woman with double vision.
***A*, Coronal contrast-enhanced CT scan shows uniformly enhancing smooth mass with associated remodeling of lateral wall of sphenoid sinus.**
***B*, T1-weighted coronal MR image defines mass as uniform region of almost absent signal, consistent with flowing blood.**
***C*, Lateral left internal carotid angiogram shows large cavernous carotid aneurysm.**

sinus was scanned with 3-mm cuts in 11 patients and 5-mm cuts in 10 patients.

MR was performed on a GE superconducting unit operating at 1.5 T. Coronal spin-echo T1-weighted images, 600–800/20 (TR/TE), were obtained in all patients with a 128 × 256 or 256^2 acquisition matrix, a 12- to 20-cm field of view, two to six excitations, a 3- to 5-mm slice thickness, and a 1- to 2.5-mm interslice skip factor. Long TR intermediate or T2-weighted images, 2500/25,50,75,100, were obtained in the coronal plane in 12 patients and in the axial plane in nine patients with a 5-mm slice thickness, 1- to 2.5-mm skip factor, 128 × 256 acquisition matrix, and 16- to 20-cm field of view. A low-resolution T1-weighted sagittal image was usually obtained as a scout view.

Angiography was performed in 13 of the 16 patients with neoplastic masses, usually as part of a balloon test occlusion of the ipsilateral internal carotid artery [4, 6]. Angiography was performed in all patients with aneurysms.

Results

CT, MR, and angiography were each evaluated for their ability to distinguish aneurysms from other masses and for their ability to define the relationship of nonaneurysmal masses to surrounding structures.

Aneurysm vs Neoplastic Mass

Six of 21 expansions of the cavernous sinus were caused by aneurysms of the parasellar segment of the carotid artery.

Four of these aneurysms showed uniform enhancement on CT and were indistinguishable from a neoplasm such as a meningioma or nerve sheath tumor (Figs. 1A) [7, 8]. On MR, three of these four appeared as signal voids, often with associated phase-encoding artifacts and low-level internal echoes probably related to turbulent flow within the aneurysm lumen (Fig. 1B) [7, 9]. In one patient with the same CT appearance, the aneurysm lumen was of intermediate signal intensity on T1-weighted images and had mixed high- and low-intensity T2 signal (Fig. 2). At angiography this aneurysm demonstrated extremely slow flow within its lumen, which may account for the higher-level internal echoes. One giant cavernous aneurysm had rim calcification and central "target" enhancement on CT (Fig. 3). MR showed the central enhancing area as a signal void associated with phase-encoding artifacts, suggesting luminal flow. The surrounding tissue had heterogeneous signal on both T1- and T2-weighted images, representing thrombus within the aneurysm lumen (Figs. 3B and 3C). Angiography was somewhat misleading in this case because it showed fusiform dilatation of the petrous and parasellar carotid but did not demonstrate the large amount of luminal thrombus (Fig. 3D). The remaining aneurysm appeared as a ring-enhancing mass on CT and was interpreted as nonvisualization of the ipsilateral internal carotid on cerebral angiography (Fig. 4). MR showed intense signal within the mass and adjacent cavernous carotid on all pulsing sequences.

Neoplastic Masses: Relationships to Surrounding Structures

In the 16 neoplastic masses, each imaging method was evaluated for its ability to depict the relationships of the mass to the carotid arteries, cranial nerves III–VI, the optic chiasm/infundibulum, the sphenoid sinus, and the bone of the skull base.

Carotid artery.—Angiography, CT, and MR were compared for their ability to demonstrate carotid displacement by tumor (Fig. 5). MR of a parasellar mass allows for simultaneous visualization of the mass and both carotid arteries. This facilitates determination of arterial displacement or encasement by tumor. Normal variation, anatomic overlap, and lack of simultaneous bilateral opacification makes visualization of subtle cavernous carotid displacement difficult on angiography (Fig. 5). Although angiography can demonstrate neoplastic narrowing occurring with advanced carotid encasement (Fig. 6) [10], encasement not resulting in narrowing was not apparent on angiography but was easily seen with MR (Fig. 7). CT was ineffective in demonstrating displacement or en-

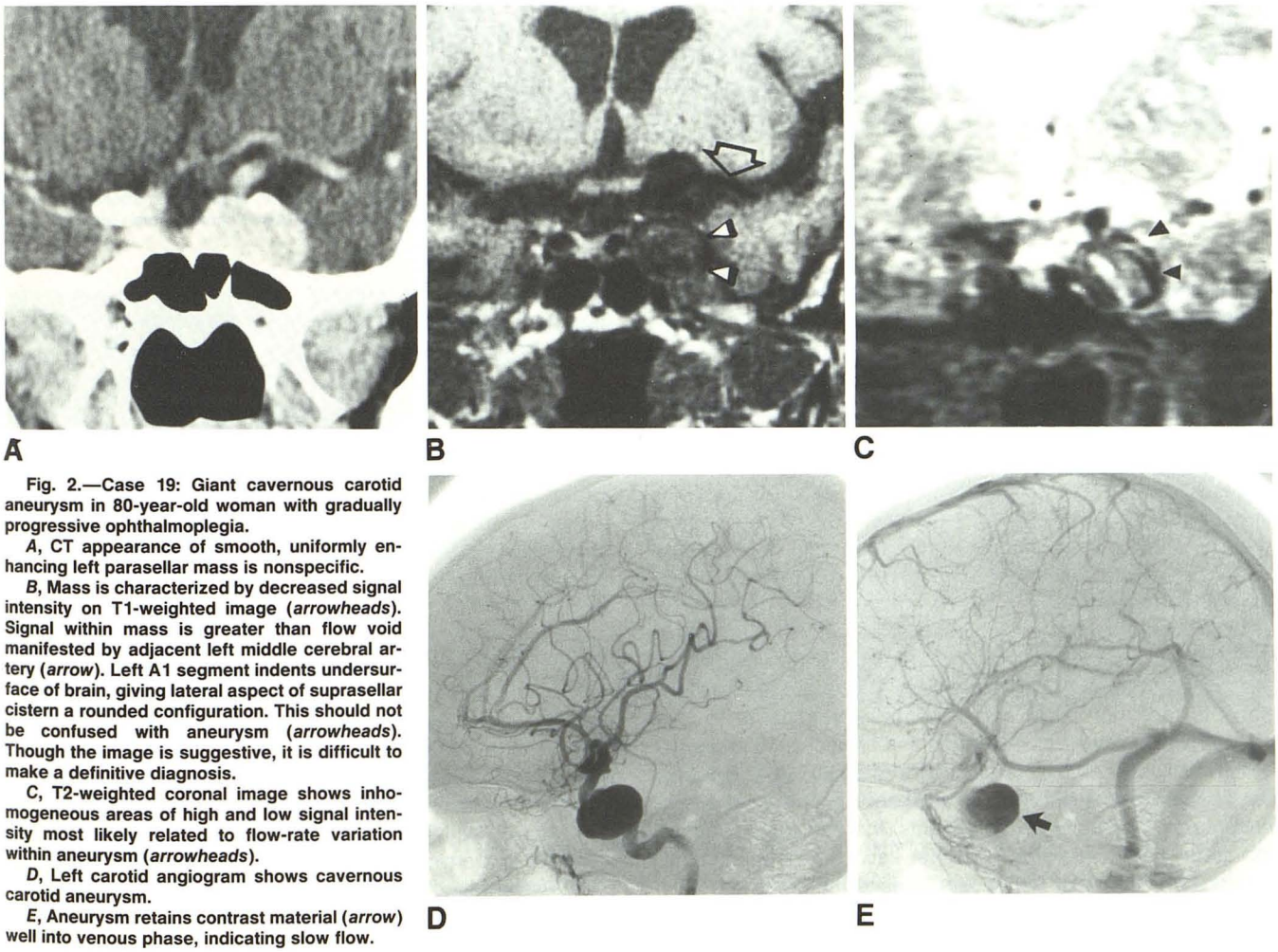

Fig. 2.—Case 19: Giant cavernous carotid aneurysm in 80-year-old woman with gradually progressive ophthalmoplegia.

***A*, CT appearance of smooth, uniformly enhancing left parasellar mass is nonspecific.**

***B*, Mass is characterized by decreased signal intensity on T1-weighted image (*arrowheads*). Signal within mass is greater than flow void manifested by adjacent left middle cerebral artery (*arrow*). Left A1 segment indents undersurface of brain, giving lateral aspect of suprasellar cistern a rounded configuration. This should not be confused with aneurysm (*arrowheads*). Though the image is suggestive, it is difficult to make a definitive diagnosis.**

***C*, T2-weighted coronal image shows inhomogeneous areas of high and low signal intensity most likely related to flow-rate variation within aneurysm (*arrowheads*).**

***D*, Left carotid angiogram shows cavernous carotid aneurysm.**

***E*, Aneurysm retains contrast material (*arrow*) well into venous phase, indicating slow flow.**

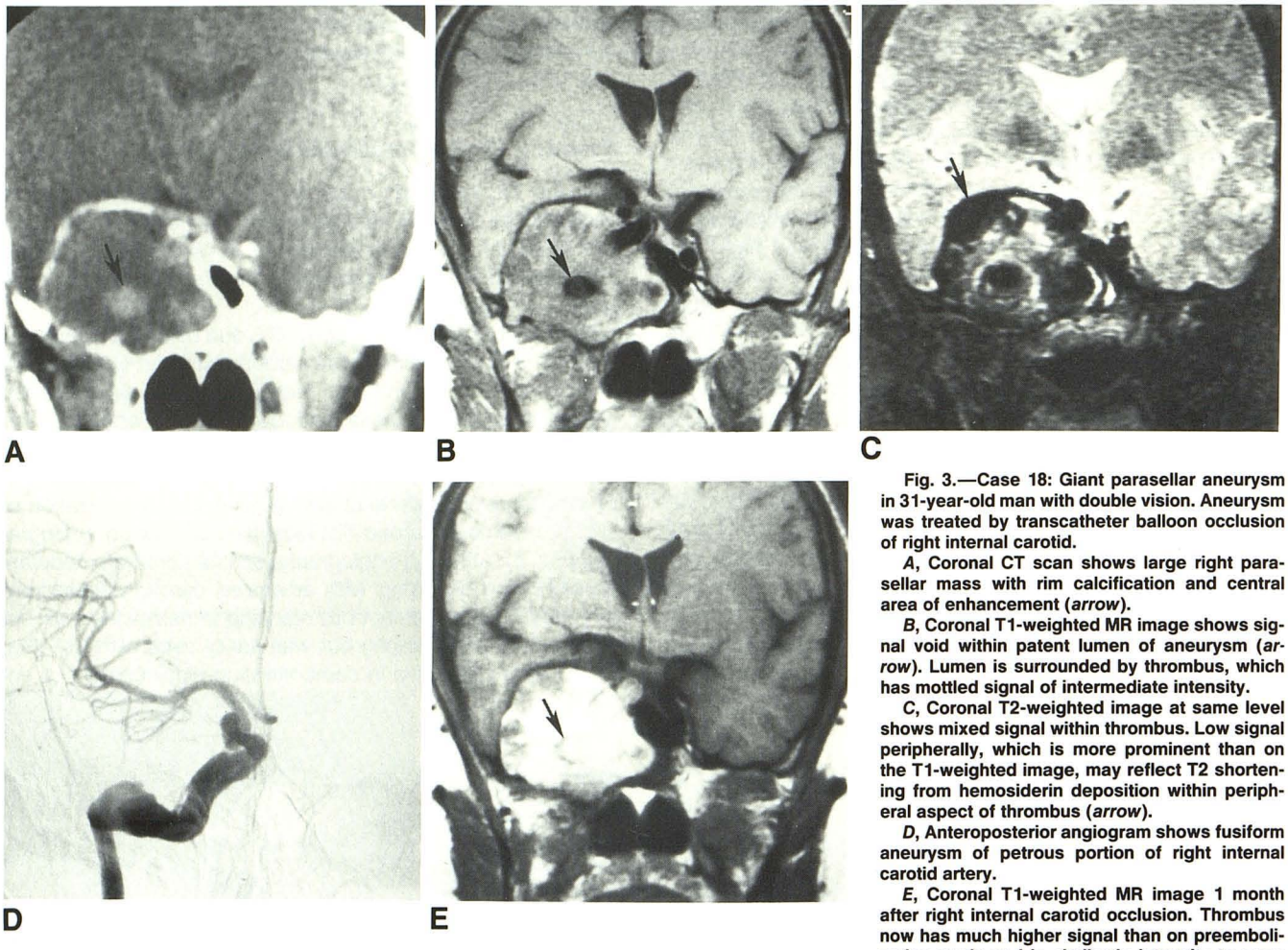

Fig. 3.—Case 18: Giant parasellar aneurysm in 31-year-old man with double vision. Aneurysm was treated by transcatheter balloon occlusion of right internal carotid.

***A*, Coronal CT scan shows large right parasellar mass with rim calcification and central area of enhancement (*arrow*).**

***B*, Coronal T1-weighted MR image shows signal void within patent lumen of aneurysm (*arrow*). Lumen is surrounded by thrombus, which has mottled signal of intermediate intensity.**

***C*, Coronal T2-weighted image at same level shows mixed signal within thrombus. Low signal peripherally, which is more prominent than on the T1-weighted image, may reflect T2 shortening from hemosiderin deposition within peripheral aspect of thrombus (*arrow*).**

***D*, Anteroposterior angiogram shows fusiform aneurysm of petrous portion of right internal carotid artery.**

***E*, Coronal T1-weighted MR image 1 month after right internal carotid occlusion. Thrombus now has much higher signal than on preembolization study and is similar in intensity to more recent thrombus in carotid lumen (*arrow*).**

casement of the carotid because of concomitant enhancement of the carotid, the cavernous sinus, and the mass itself (Fig. 5).

Cranial nerves.—In the 16 neoplasms studied, the ipsilateral intracavernous segments of cranial nerves III, IV, and VI were not identified in any case by MR or CT. In contrast, Meckel cave, which contains V_1 and sometimes V_2, was routinely demonstrated by both methods. This CSF-filled reflection of dura was routinely seen on enhanced CT as a low density within the posterior inferior aspect of the enhanced cavernous sinus (Fig. 8A). On T1-weighted images, Meckel cave appeared as a focal area of low signal intensity (Fig. 8B), and on T2-weighted images it had high signal intensity similar to CSF (Fig. 8C). Ipsilateral to the mass, Meckel cave was completely effaced in 10 patients, partially compressed in four patients, and normal in two patients. Contralateral to the mass, Meckel cave was visualized and normal in 15 patients, but partially effaced by a large chondrosarcoma (that crossed the midline) in one patient. Identical findings were noted on enhanced CT scanning in 13 patients. In three cases, neither ipsilateral nor contralateral Meckel cave could be demonstrated by CT despite 5-mm cuts through the area.

Dural reflections of the cavernous sinus.—On CT, the dural reflection forming the lateral wall of the cavernous sinus was identified as a thin rim of enhancement surrounding the tumor [10]. This was seen in eight of 16 patients. On MR, the lateral dural reflection appeared as a thin rim of low signal adjacent to the mass on T1-weighted images (Fig. 8B). This rim was visible in all patients, but was incomplete in four: three previously operated meningiomas and one large pituitary adenoma that invaded the temporal lobe. The lateral wall of the cavernous sinus was convex laterally (bulging) in all of the cavernous sinus neoplasms studied. Early involvement of the cavernous sinus by neoplasm without bulging in the lateral wall was not observed. In contrast to the excellent demonstration of the lateral wall of the cavernous sinus, the medial wall bordering the pituitary fossa was not seen in any patient.

Optic chiasm/infundibulum.—The optic chiasm and infundibulum were demonstrated more reliably on MR than on CT. With MR the chiasm was identified in 16 of 16 patients with parasellar neoplasms, whereas CT delineated the chiasm in 13 of 16 patients. The infundibulum was identified in all patients with both MR and CT. Because of increased contrast with MR, anatomic definition of both the chiasm and infundibulum was superior to CT [11].

Sphenoid sinus and skull base.—The one area where CT

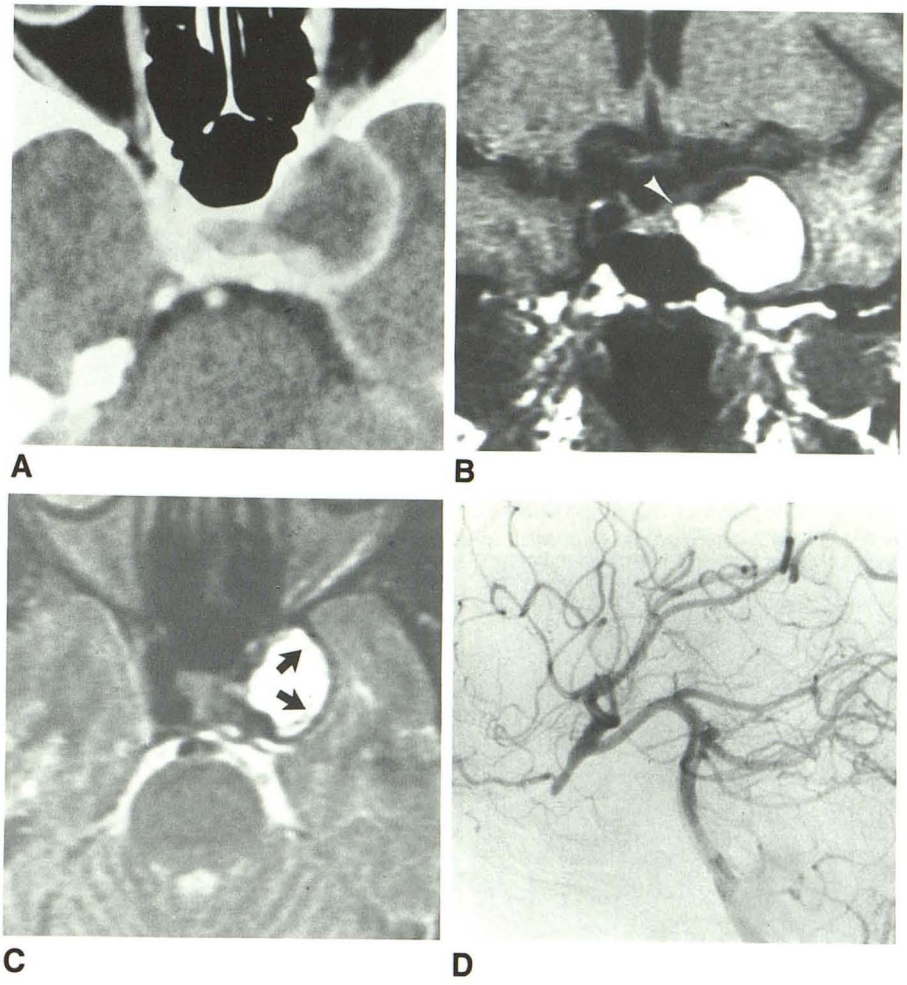

Fig. 4.—Case 20: Thrombosed aneurysm in 49-year-old woman with 2-week history of periorbital pain and left sixth nerve palsy.

A, Axial contrast-enhanced CT scan delineates ring-enhancing left parasellar mass.

B, Coronal T1-weighted image illustrates largely hyperintense mass consistent with subacute thrombus. Note thrombosed portion of adjacent left cavernous internal carotid artery (*arrowhead*).

C, Axial T2-weighted image. Mass remains primarily hyperintense, with well-defined internal ring of decreased signal intensity, illustrating laminar composition (*arrows*).

D, Left vertebral angiogram shows filling of left middle cerebral artery and left internal carotid artery (supraclinoid portion). Injection of both common carotid arteries also failed to show aneurysm.

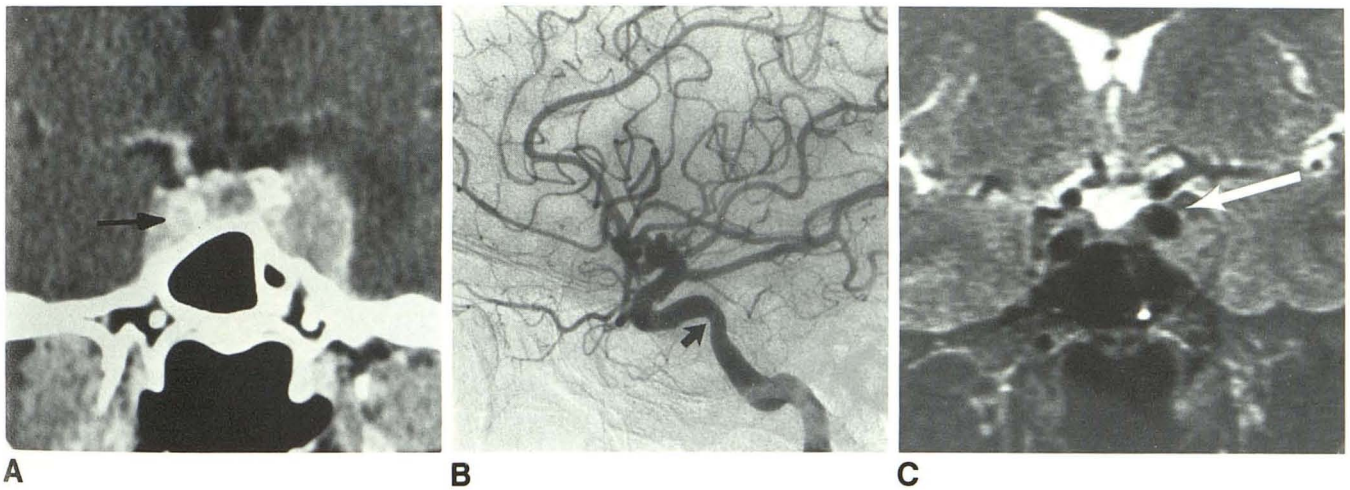

Fig. 5.—Case 2: Left parasellar meningioma in 63-year-old woman with 1½-year history of left facial pain.

A, Coronal CT scan shows a uniformly enhancing left parasellar mass. Left cavernous carotid artery cannot be identified. Incidently noted is calcification in contralateral right cavernous carotid artery (*arrow*).

B, Lateral left carotid angiogram defines cavernous carotid. There is subtle superior displacement of cavernous segment and a question of narrowing of precavernous segment (*arrow*).

C, Coronal T2-weighted MR image clearly shows that left cavernous carotid artery (*arrow*) is superiorly displaced by isointense meningioma.

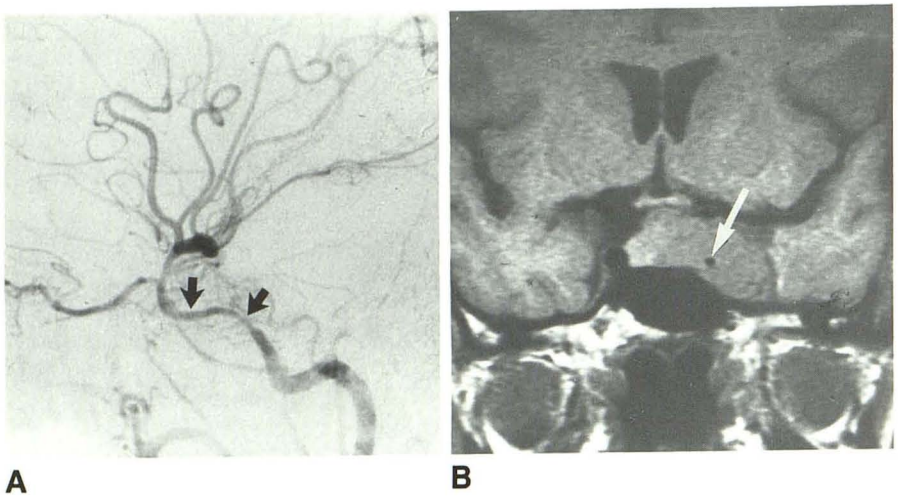

Fig. 6.—Case 7: 36-year-old woman with recurrent left cavernous sinus meningioma.

A, Lateral left carotid angiogram shows narrowing of cavernous and precavernous internal carotid artery secondary to encasement (*arrows*).

B, Slightly hypointense meningioma on T1-weighted image encases cavernous carotid, which is seen as small circular flow void (*arrow*).

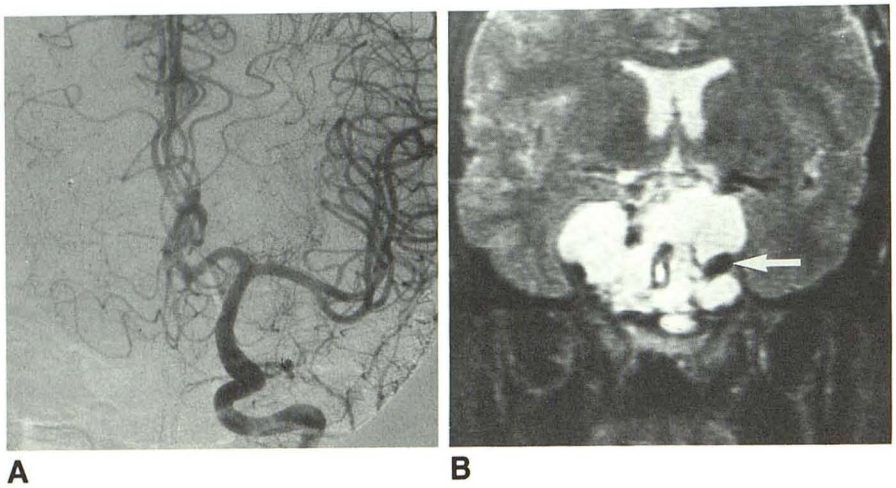

Fig. 7.—Case 14: 25-year-old man with recurrent chondrosarcoma.

A, Anteroposterior left carotid angiogram shows uncoiling of carotid siphon without evidence of luminal narrowing.

B, T2-weighted coronal image shows cavernous carotid (*arrow*) almost totally engulfed by tumor, which has very intense signal characteristics.

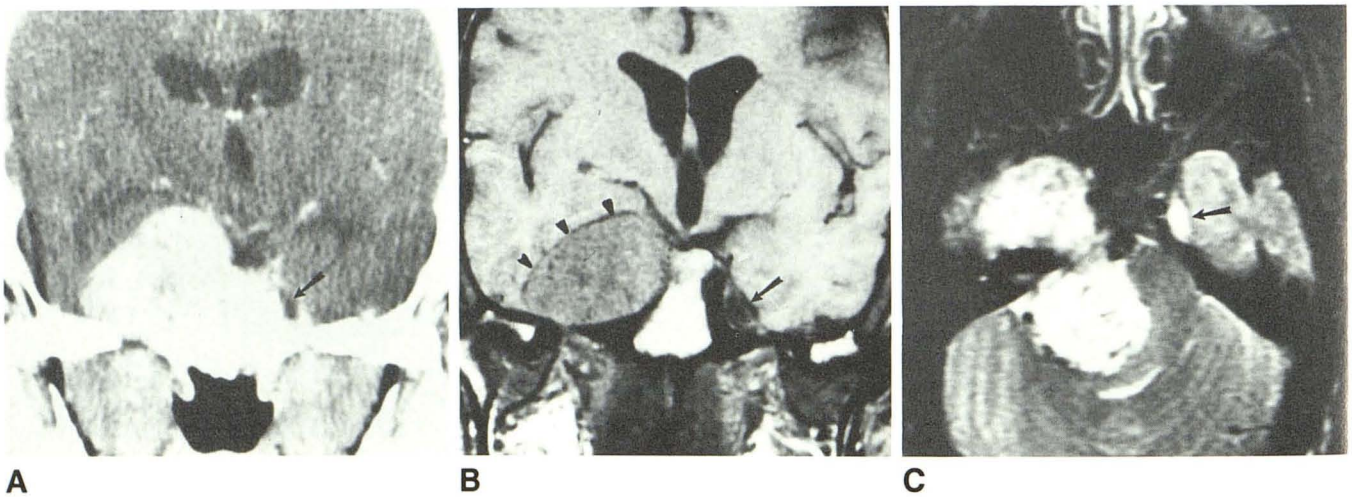

Fig. 8.—Case 11: Large fifth nerve sheath tumor ("trigeminal neuroma") in 31-year-old man with deteriorating mental status and hydrocephalus.

A, Coronal contrast-enhanced CT scan shows large, uniformly enhancing mass in right cavernous sinus. Meckel cave is completely effaced on right and is normal on left (*arrow*).

B, T1-weighted coronal image shows mass to be slightly hypointense relative to brain. Low-signal rim (*arrowheads*) may represent dural reflection forming lateral margin of cavernous sinus. Meckel cave is obliterated on right by tumor. Note normal appearance of Meckel cave on left (*arrow*).

C, Axial T2-weighted image. Mass is markedly hyperintense relative to brain. Note intense signal in normal left Meckel cave (*arrow*).

This case illustrates that on T2-weighted images a small fifth nerve sheath tumor may be missed because it can have signal characteristics similar to CSF, which normally occupies Meckel cave.

was clearly superior to MR was in the evaluation of bone changes adjacent to cavernous sinus masses. In 16 patients with neoplastic masses, MR showed gross invasion of the sphenoid sinus in four, remodeling of the sellar floor in three, a hypoplastic sphenoid sinus in one, and no abnormality in eight. CT findings were identical to those of MR except in one pituitary adenoma with erosion of the anterior sellar floor, a potentially helpful finding not visible on MR (Fig. 9).

Hyperostosis was detected by CT in five of seven cavernous meningiomas. Corresponding MR scans were reviewed to look for bone changes consistent with hyperostosis (thickening of contour, indistinctness of cortical margins, increased marrow signal) [12]. Retrospectively, MR demonstrated bone changes in all five of these patients (Fig. 10).

Signal Characteristics of Parasellar Masses

Of the seven meningiomas, T1-weighted images showed six to be isointense relative to brain, and one was minimally hypointense. On T2-weighted images, six meningiomas were isointense and one was hyperintense. All three pituitary macroadenomas were isointense relative to brain on T1- and T2-weighted images. Neoplasms other than meningiomas and pituitary adenomas were hypointense on T1- and hyperintense on T2-weighted images [13].

Discussion

Recent advances in technique allow successful surgical removal of masses involving the cavernous sinus, often without impairment of cranial nerve function and with preservation of patency of the carotid artery. Prior to this extensive surgery, imaging is used to exclude aneurysm and to determine the relationship of parasellar neoplasms to the cavernous carotid; the optic chiasm; cranial nerves III, IV, V, and VI; the pituitary gland; and the bone surrounding the parasellar region [3, 4].

MR is superior to drip-infusion CT in differentiating giant cavernous aneurysms from neoplasms (Figs. 1 and 2). However, the diagnostic accuracy of CT is dramatically improved

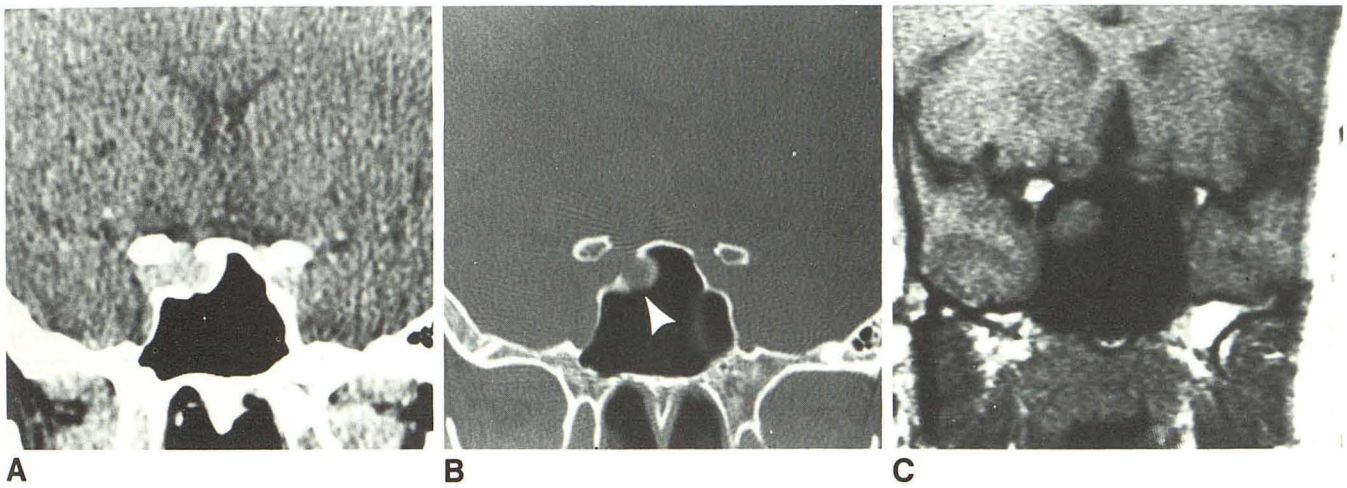

Fig. 9.—Case 10: Pituitary adenoma in 48-year-old man with elevated prolactin levels.
***A*, Contrast-enhanced 1.5-mm-thick coronal CT scan shows focal remodeling of anterior aspect of sella caused by pituitary adenoma.**
***B*, Bone algorithm delineates thinning of wall of sphenoid adjacent to adenoma (*arrowhead*).**
***C*, Coronal T1-weighted image through same region shows adenoma, but adjacent bone cannot be distinguished from air in sphenoid sinus.**

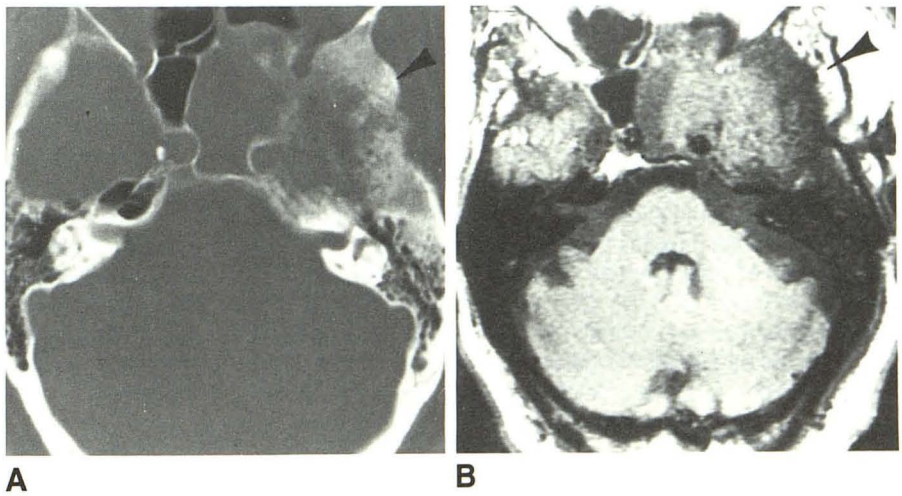

Fig. 10.—Case 6: Recurrent meningioma in 63-year-old man.
***A*, Axial CT scan with bone algorithm shows hyperostosis of left sphenoid and temporal bones (*arrowhead*).**
***B*, Comparable axial T1-weighted MR image. Hyperostotic bone of floor of left temporal fossa (*arrowhead*) is visibly thickened and has higher signal than normal bone. CT and MR images were both obtained at level of internal auditory canals.**

by using dynamic scanning and bolus injection of contrast material [14]. With this technique, CT and MR probably are of nearly equal efficacy in differentiating neoplastic and aneurysmal parasellar masses. MR and dynamic contrast CT have advantages over angiography in the evaluation of some parasellar aneurysms, specifically those that are partially or completely thrombosed. In partially thrombosed aneurysms, angiography underestimates aneurysm size by showing only the lumen, while MR and CT demonstrate the lumen and the mural clot (Fig. 3). Completely thrombosed aneurysms, which appear as a nonspecific blush on angiography and as a ring-enhancing mass on CT, are best characterized on MR (Fig. 4). Despite the success of MR in the evaluation of giant aneurysms, several pitfalls in diagnosis remain. Small (<1 cm) cavernous aneurysms can be difficult to distinguish from normal tortuosity of the cavernous carotid. Flow-rate variation in large patent aneurysms results in a wide spectrum of signal characteristics within the lumen. These range from a signal void when flow is rapid (Fig. 1B) to an isointense or even hyperintense signal (Figs. 2B and 2C) when flow within the aneurysm lumen is slow or turbulent. In ambiguous cases dynamic contrast bolus CT or angiography may be required for diagnosis. Low-flip-angle gradient-recalled echo sequences also may be a reliable method of differentiating a solid mass from slow or turbulent flow within giant aneurysms, but this will have to be substantiated. Another potential problem is that the signal of clot within a completely or partially thrombosed aneurysm may vary considerably depending on its age and the presence of an adjacent patent vascular lumen (Figs. 3B, 3C, and 3E). Because of this variation, it is conceivable that the signal characteristics of clot may be similar to those of a neoplastic mass. Hemorrhagic neoplasms might also be confused with aneurysm [7].

In the evaluation of cavernous sinus neoplasms, MR is generally more informative than CT, particularly in establishing the relationship of the neoplasm to surrounding structures. T1-weighted coronal images were the most valuable imaging sequence. The relationships of the parasellar masses to the carotid, pituitary fossa, suprasellar cistern, medial temporal lobe, sphenoid sinus, and Meckel cave were all well demonstrated. Cavernous sinus masses may displace cranial nerves within the cavernous sinus in any direction, and preoperative visualization is useful in surgical planning. Cranial nerves III, IV, V_1, and sometimes V_2 are intimately related to the lateral wall of the cavernous sinus, and cranial nerve VI runs within the sinus itself [2]. The intracavernous segments of cranial nerves III, IV, and VI were not visualized ipsilateral to the mass with either CT or MR in any patient in our series, possibly because of effacement by the adjacent mass. These nerves often are so attenuated that they are not visible at surgery, and can only be demonstrated intraoperatively by direct electrical stimulation and electromyographic monitoring of the extraocular muscles [3]. In the normal cavernous sinus, visualization of cranial nerves III, IV, and VI has been reported on both MR and CT [15]. Our preliminary experience with gadolinium-enhanced coronal T1-weighted images suggests that they will be superior to coronal CT and unenhanced MR in the definition of these cranial nerves in normal subjects. It may remain difficult, however, to demonstrate these structures in the presence of a large cavernous sinus mass.

The T2 signal characteristics of parasellar neoplasms were useful in limiting the differential diagnosis. In this small series six of seven parasellar meningiomas and the three pituitary macroadenomas involving the cavernous sinus were hypointense or isointense on T1- and T2-weighted sequences (relative to white matter). Similar findings have been observed by others [12, 13]. The six parasellar neoplasms with other histologies all had low T1 and high T2 signal intensities. Signal characteristics, however, are of limited specificity. Some meningiomas have increased T2 signal intensity, and these will be difficult to differentiate from other parasellar masses on the basis of signal characteristics alone [12]. Pituitary macroadenomas also can have variable signal characteristics, particularly if they are cavitated [16, 17].

A limitation of both CT and MR is the recognition of very small parasellar neoplasms that do not distort the contour of the cavernous sinus but are still able to produce symptoms, usually a cranial nerve palsy. In particular, small isointense meningiomas might be overlooked by MR. In such cases CT may be helpful because of its superb sensitivity to calcification and hyperostosis. While MR did show evidence of hyperostosis in five of seven meningiomas, this analysis was retrospective. The ability of MR to prospectively detect hyperostosis without benefit of comparison CT remains to be established.

In patients with signs of a parasellar lesion (such as unilateral ophthalmoplegia, sensory deficits in the V_1 and V_2 distribution, and retroorbital pain) [18], both enhanced CT and MR directed at examining the parasellar region (coronal plane, 3- to 5-mm cuts through area) are capable of detecting most parasellar masses. Angiography does little in narrowing the differential diagnosis of neoplasms, and aneurysm can usually be diagnosed noninvasively by using MR or dynamic bolus-contrast CT [4, 5, 7]. However, when surgical intervention is considered, angiography still provides anatomic information not available with other methods, such as tumor vascularity [10] and the characterization of the neck of aneurysms. We also advocate transcatheter balloon test occlusion of the ipsilateral carotid artery prior to cavernous sinus surgery, believing that test occlusion is helpful in predicting which patients can tolerate sacrifice of the carotid artery, whether it is intentional or is a complication of cavernous sinus surgery [4]. The usefulness of this later procedure is currently being reviewed. Interventional neuroradiology also plays an increasing role in treatment. Occlusion of the lumen or parent vessel with detachable balloons has become the treatment of choice for giant parasellar aneurysms in some centers [5, 19].

In summary, when available, MR should be the initial diagnostic method in the evaluation of patients with suspected parasellar masses. The advantages of MR are first in deciding whether the lesion is an aneurysm or neoplasm and, second, in defining the regional anatomic relationships more accurately than can be accomplished with CT. Angiography and CT will continue to have important supplementary roles in the evaluation of these masses, particularly when surgical intervention is planned.

ACKNOWLEDGMENT

We thank Dara Tomassi for preparing and editing the manuscript.

REFERENCES

1. Taptas JN. The so-called cavernous sinus: a review of the controversy and its implications for neurosurgeons. *Neurosurgery* **1982**;11(5):712–716
2. Umansky F, Nathan H. The lateral wall of the cavernous sinus. *J Neurosurg* **1982**;56:228–234
3. Sekhar L, Moller A. Operative management of tumors involving the cavernous sinus. *J Neurosurg* **1986**;64:879–889
4. Sekhar L, Schramm V, Jones N, et al. Operative exposure and management of the petrous and upper cervical internal carotid artery. *Neurosurgery* **1986**;19(6):967–982
5. Raymond J, Theron J. Intracavernous aneurysms, treatment by proximal occlusion of the internal carotid artery. *AJNR* **1986**;7:1087–1092
6. Spetzler RF, Carter LP. Revascularization and aneurysm surgery: current status (review article). *Neurosurgery* **1985**;16(1):111–116
7. Olsen W, Brant-Zawadzki M, Hodes J, Norman D, Newton T. Giant intracranial aneurysms: MR imaging. *Radiology* **1987**;163:431–435
8. Pinto R, Kricheff I, Butler A, Murali R. Correlation of computed tomographic, angiographic, and neuropathological changes in giant cerebral aneurysms. *Radiology* **1979**;132:85–92
9. Atlas S, Grossman R, Goldberg H, Hackney D, Bilaniuk L, Zimmerman R. Partially thrombosed giant intracranial aneurysms: correlation of MR and pathologic findings. *Radiology* **1987**;162:111–114
10. Moore T, Ganti SR, Mowad M, Hilal S. CT and angiography of primary extradural juxtasellar tumors. *AJNR* **1985**;145:491–496
11. Karmaze M, Sartor K, Winthrop J, Gado M, Hodges F. Suprasellar lesions: evaluation with MR imaging. *Radiology* **1986**;161:77–82
12. Zimmerman R, Fleming C, Saint-Louis L, Lee B, Manning J, Deck M. Magnetic resonance imaging of meningiomas. *AJNR* **1985**;6:149–157
13. Lee B, Deck M. Sellar and juxtasellar lesion detection with MR. *Radiology* **1985**;157:143–147
14. Pinto PS, Cohen WA, Kricheff I. Giant intracranial aneurysms: rapid sequential computed tomography. *AJNR* **1982**;3:495–499
15. Daniels DL, Pech P, Mark L, Pojunas K, Williams A, Haughton V. Magnetic resonance imaging of the cavernous sinus. *AJNR* **1985**;6:187–192
16. Davis P, Hoffman J, Spencer T, Tindall G, Braun I. MR imaging of pituitary adenoma: CT, clinical, and surgical correlation. *AJR* **1987**;148:797–802
17. Kucharczyk W, Davis D, Kelly W, Sze G, Norman D, Newton T. Pituitary adenomas: high resolution MR imaging at 1.5 T. *Radiology* **1986**;161:761–765
18. Thomas Y, Yoss R. The parasellar syndrome: problems in determining etiology. *Mayo Clin Proc* **1970**;45:617–623
19. Hieshima G, Higashida R, Halbach V, Cahan L, Goto K. Intravascular balloon embolization of a carotid-ophthalmic artery aneurysm with preservation of the parent vessel. *AJNR* **1986**;7:916–918